Enantiospecific state transfer for gaseous symmetric-top chiral molecules

Bo Liu [1] Chong Ye,[2,1] C. P. Sun,[1,3] and Yong Li[1,4,*]

[1]*Beijing Computational Science Research Center, Beijing 100193, China*
[2]*Beijing Key Laboratory of Nanophotonics and Ultrafine Optoelectronic Systems School of Physics,*
Beijing Institute of Technology, Beijing 100081, China
[3]*Graduate School of China Academy of Engineering Physics, Beijing 100193, China*
[4]*Center for Theoretical Physics and School of Science, Hainan University, Haikou 570228, China*

We study the enantiospecific state transfer for gaseous symmetric-top chiral molecules by constructing a four-level model. This model is formed by coupling the electric dipole transitions among four appropriate rovibrational states with three electromagnetic fields. It includes two cyclic three-level substructures, where the overall phases of the coupling strengths differ by π with enantiomers and reflect the chirality dependence of the molecules. Based on this four-level model, two dynamic ways are proposed to achieve the approximately perfect enantiospecific state transfer for gaseous symmetric-top chiral molecules when all the molecules are initially in the ground state of the system.

I. INTRODUCTION

A chiral molecule is not superposable on its mirror image through pure translation and/or rotation. The left- and right-handed chiral molecules (called enantiomers) coexist in many biologically active compounds and may have significant differences in physiological effects, pharmacological effects, and biological processes [1–3]. Only one enantiomeric form is biologically beneficial, while the other one may be harmful or fatal. Thus, the enantiodetection, enantioseparation, and enantioconversion of chiral molecules are important and challenging tasks [4–14].

In the past few decades, the research of chiral molecules based on a cyclic three-level configuration via electric dipole transitions [15–34] has become remarkable in the physics of atomic, molecular, and optical physics. For natural atoms, such a cyclic three-level system is forbidden, because three electric dipole transitions cannot coexist due to the electric dipole selection rules. However, the cyclic three-level system can exist in chiral molecules and other symmetry-broken systems [35–37]. Due to the intrinsic property of chiral molecules, the product of the corresponding three electric dipoles of the enantiomer in the cyclic three-level model differs in sign. So the overall phase of the product of three coupling strengths in the cyclic three-level model of the enantiomer differs by π. The chirality dependence of the overall phase makes the dynamics of enantiomers different. Based on this fact, theoretical methods for enantiospecific state transfer [18–24], enantiodetection [25–32], and enantioseparation [33,34] of chiral molecules were proposed.

For gaseous molecules, the rotational degrees of freedom of the molecule should be involved [38–56]. Chiral molecules can be assumed to be rigid enough to describe their rotation by the Hamiltonian of the symmetric or asymmetric top [38]. Due to the magnetic degeneracy of the molecular rotational states, the ideal single-loop cyclic three-level model in the original schemes [15–34] is generally replaced by a complicated multiple-loop three-level model, where each level may be composed of multiple degenerate levels with different magnetic quantum numbers [39,40]. Some experimental groups have utilized such a multiple-loop three-level model to realize enantiospecific state transfer [40] (as well as enantiodetection [40–48]) for gaseous chiral molecules. It was pointed out [40] that this multiple-loop three-level configuration limits the experimental efficiency. Therefore, in order to improve the efficiency of enantiospecific state transfer (as well as enantiodetection), it is necessary to select a real few-level model, where each level does not consist of degenerate levels with different magnetic quantum numbers.

For gaseous asymmetric-top chiral molecules, further investigations [49,50] pointed out that the ideal single-loop cyclic three-level model can be formed by applying three appropriate electromagnetic fields. In such an ideal single-loop cyclic three-level model, recently the enantiospecific state transfer has been achieved experimentally [51] for asymmetric-top molecules with much better enantiomer enrichment compared with previous works [40,41] by depleting the thermal population in one of the excited levels of the cyclic three-level model. In addition, in order to realize the enantiospecific state transfer of asymmetric-top chiral molecules initially distributed over magnetic degenerate states, the theoretical method of synchronizing several isolated cyclic three-level subsystems was proposed [52].

Different from the case of asymmetric-top chiral molecules, for gaseous symmetric-top chiral molecules, it is impossible to form the ideal chirality-dependent single-loop cyclic three-level model due to their electric

---

*liyong@csrc.ac.cn

dipole selection rules [39]. Note that the controllability of rotational dynamics of symmetric-top chiral molecules was recently studied theoretically [53,54]. The controllability could take an important role in the rotational state-selective excitation of chiral molecules [53,54]. However, Refs. [53,54] focused on studying the controllability of rotational dynamics of symmetric-top chiral molecules, instead of constructing specific chirality-dependent single-loop few-level models and achieving the enantiospecific state transfer (or enantioseparation) for symmetric-top chiral molecules.

In this paper, for gaseous symmetric-top chiral molecules, we construct a simple chirality-dependent four-level model to achieve the approximately perfect enantiospecific state transfer. Our four-level model includes two cyclic three-level substructures, formed by selecting appropriately the rovibrational states and the corresponding three electromagnetic fields based on the electric dipole selection rules of symmetric-top chiral molecules. In each cyclic three-level substructure, the product of the corresponding three electric dipoles changes sign with enantiomers. That is, the overall phase of the coupling strengths in each cyclic three-level substructure differs by π with enantiomers, which reflects the chirality dependence of this model and shows different dynamics for enantiomers. Thus, enantiospecific state transfer (as well as enantiodetection and enantioseparation) can be achieved by using such dynamical differences. For simplicity, under the large-detuning condition, we further reduce the four-level model to an effective two-level one with the same detuning but different effective couplings for enantiomers. Then we realize the approximately perfect enantiospecific state transfer for symmetric-top chiral molecules in two dynamic ways. Thereby, enantiopure molecules can be further spatially separated from the initial chiral mixture by a variety of energy-dependent processes [33,34,57].

The structure of the article is as follows. In Sec. II we introduce the electric dipole rovibrational transition of symmetric-top chiral molecules. In Sec. III the four-level model with two cyclic three-level substructures is realized for symmetric-top chiral molecules by applying three electromagnetic fields. In Sec. IV, taking the D_2S_2 molecule as an example, we show how to choose the vibrational wave functions of the working states. In Sec. V, based on the four-level model, two dynamic ways are used to achieve the enantiospecific state transfer for symmetric-top chiral molecules. A summary and conclusions are given in Sec. VI.

II. ELECTRIC DIPOLE ROVIBRATIONAL TRANSITION OF SYMMETRIC-TOP CHIRAL MOLECULES

The rotational Hamiltonian for a chiral molecule reads ($\hbar = 1$) [38]

$$\hat{H}_{\text{rot}} = A\hat{J}_z^2 + B\hat{J}_x^2 + C\hat{J}_y^2, \tag{1}$$

with three rotational constants A, B, and C. In the following, we focus on the prolate symmetric-top chiral molecules ($A > B = C$). Here $\hat{J}_{x,y,z}$ are angular momentum operators along the principal axes of the moment of inertia, respectively. The eigenstates of the rotational Hamiltonian (1) are $|J, K, M\rangle$ with the total angular momentum number J, the quantum

number K ($-J \leqslant K \leqslant J$), and the magnetic quantum number M ($-J \leqslant M \leqslant J$). Here K and M are the projections of the angular momentum on the molecule-fixed z axis and the space-fixed Z axis, respectively. The corresponding eigenenergies are $\varepsilon_{J,K} = CJ(J+1) + (A-C)K^2$ [38].

In the following discussion, we suppose that the coupling among vibration, rotation, and electronic wave functions of the molecule can be neglected. To elucidate our scheme simply, we assume all the working states are in the electronic ground state and omit it later. Then the full wave function of the chiral molecule can be described by the basis $\{|l\rangle = |v_l\rangle \otimes |J_l, K_l, M_l\rangle\}$, with $|v_l\rangle$ the vibrational wave functions.

On the other hand, an electromagnetic field can be written in the linear combination $\mathbf{E}^s = \text{Re}\{\sum_{\sigma=0,\pm1} \boldsymbol{e}_\sigma^s E_\sigma^s e^{-i(\omega t + \varphi_\sigma)}\}$. The symbol s indicates the space-fixed frame; E_σ^s, ω, and φ_σ are the field amplitude, the frequency, and the initial phase of the electromagnetic field, respectively; σ indicates the helicity component of the electromagnetic field with $\boldsymbol{e}_0^s = \boldsymbol{e}_Z^s$ and $\boldsymbol{e}_{\pm1}^s = (i\boldsymbol{e}_Y^s \pm \boldsymbol{e}_X^s)/\sqrt{2}$; and $\boldsymbol{e}_X^s$, $\boldsymbol{e}_Y^s$, and $\boldsymbol{e}_Z^s$ correspond to the unit vectors of axes of the space-fixed frame.

For the electric dipole-allowed transition between a lower level $|l\rangle$ and an upper level $|j\rangle$, the interaction Hamiltonian $\hat{V}^s = \hat{\boldsymbol{\mu}} \cdot \mathbf{E}^s$ is obviously written as $\hat{V}^s = \Omega_{jl} e^{-i\omega t} |j\rangle\langle l| +$ H.c. ($j > l$) [39,49], where $\hat{\boldsymbol{\mu}}$ is the electric dipole operator and Ω_{jl} is the coupling strength

$$\Omega_{jl} = \frac{1}{2} \sum_{\sigma=0,\pm1} E_\sigma^s e^{-i\varphi_\sigma} \langle j|\hat{\mu}_\sigma^s|l\rangle$$

$$= \frac{1}{2} \sum_{\sigma,\sigma'=0,\pm1} \sqrt{(2J_j+1)(2J_l+1)} \langle v_j|\hat{\mu}_{\sigma'}^m|v_l\rangle E_\sigma^s$$

$$\times (-1)^{\sigma+\sigma'-K_l+M_l} e^{-i\varphi_\sigma} W_{J_jM_j,J_lM_l}^{(\sigma)} W_{J_jK_j,J_lK_l}^{(\sigma')}. \tag{2}$$

Here $\hat{\mu}_\sigma^s = \hat{\boldsymbol{\mu}} \cdot \boldsymbol{e}_\sigma^s$ and $\hat{\mu}_{\sigma'}^m = \hat{\boldsymbol{\mu}} \cdot \boldsymbol{e}_{\sigma'}^m$ are the components of the electric dipole in the space-fixed frame and the molecule-fixed frame, respectively, σ' indicates the spherical components of the electric dipole $\hat{\mu}_{\sigma'}^m$ in the molecule-fixed frame with $\boldsymbol{e}_0^m = \boldsymbol{e}_z^m$ and $\boldsymbol{e}_{\pm1}^m = (i\boldsymbol{e}_y^m \pm \boldsymbol{e}_x^m)/\sqrt{2}$, and $\boldsymbol{e}_{x,y,z}^m$ correspond to the unit vectors of axes of the molecule-fixed frame. Here the $3j$ symbol reads

$$W_{JM,J'M'}^{(\sigma)} = \begin{pmatrix} J & 1 & J' \\ M & -\sigma & -M' \end{pmatrix}. \tag{3}$$

We are interested in the condition that the coupling strengths in Eq. (2) are nonzero. The $3j$ symbols play a key role in determining the electric dipole selection rules, that is, $\Delta J = J_j - J_l = 0, \pm1$, $\Delta M = M_j - M_l = \sigma$, and $\Delta K = K_j - K_l = \sigma'$ [39]. These electric dipole selection rules offer the possibility of forming the four-level model of symmetric-top chiral molecules.

III. CHIRALITY-DEPENDENT FOUR-LEVEL CONFIGURATION

In this section we realize the chirality-dependent four-level model of symmetric-top chiral molecules by choosing appropriate states $|J, K, M\rangle$ according to the electric dipole selection rules. For simplicity, we focus on the subspace $J \leqslant 1$.
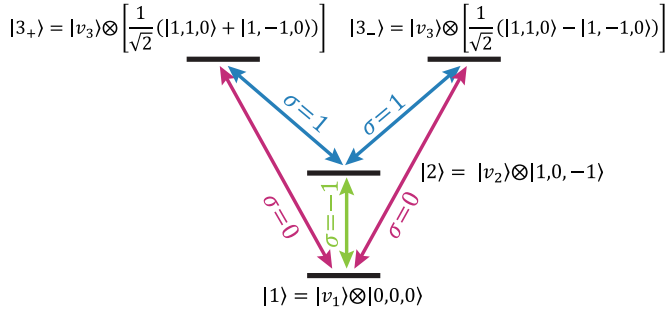
FIG. 1. Four-level model of the symmetric-top molecule. Two cyclic three-level substructures $|1\rangle \rightarrow |2\rangle \rightarrow |3_+\rangle \rightarrow |1\rangle$ and $|1\rangle \rightarrow |2\rangle \rightarrow |3_-\rangle \rightarrow |1\rangle$ coexist under the interaction with three electromagnetic fields. Here $\sigma = 0$ corresponds to the linearly Z polarized electromagnetic field with the polarization vector $\boldsymbol{e}_0^s = \boldsymbol{e}_Z^s$; $\sigma = 1$ ($\sigma = -1$) corresponds to the circularly polarized electromagnetic field rotating about the Z axis in the right-handed (left-handed) sense with the polarization vector $\boldsymbol{e}_1^s = (i\boldsymbol{e}_Y^s + \boldsymbol{e}_X^s)/\sqrt{2}$ [$\boldsymbol{e}_{-1}^s = (i\boldsymbol{e}_Y^s - \boldsymbol{e}_X^s)/\sqrt{2}$].

The working states are selected as

$$|1\rangle \equiv |v_1\rangle \otimes |0, 0, 0\rangle,$$

$$|2\rangle \equiv |v_2\rangle \otimes |1, 0, -1\rangle,$$

$$|3_+\rangle \equiv |v_3\rangle \otimes \left[\frac{1}{\sqrt{2}}(|1, 1, 0\rangle + |1, -1, 0\rangle) \right],$$

$$|3_-\rangle \equiv |v_3\rangle \otimes \left[\frac{1}{\sqrt{2}}(|1, 1, 0\rangle - |1, -1, 0\rangle) \right]. \quad (4)$$

Here, since the rotational constants for the prolate symmetric-top chiral molecules meet $B = C$, the state $|1, 1, 0\rangle$ and the state $|1, -1, 0\rangle$ are degenerate. Therefore, $|3_+\rangle$ and $|3_-\rangle$, which are the superposition states of $|1, 1, 0\rangle$ and $|1, -1, 0\rangle$, are degenerate.

Correspondingly, we select the three electromagnetic fields

$$\mathbf{E}_{12}^s = \text{Re}\left\{ \boldsymbol{e}_{-1}^s E_{12}^s e^{-i(\omega_{12}t + \varphi_{12})} \right\},$$

$$\mathbf{E}_{23}^s = \text{Re}\left\{ \boldsymbol{e}_1^s E_{23}^s e^{-i(\omega_{23}t + \varphi_{23})} \right\},$$

$$\mathbf{E}_{13}^s = \text{Re}\left\{ \boldsymbol{e}_0^s E_{13}^s e^{-i(\omega_{13}t + \varphi_{13})} \right\}. \quad (5)$$

Because $|3_+\rangle$ and $|3_-\rangle$ are degenerate, two cyclic three-level substructures $|1\rangle \rightarrow |2\rangle \rightarrow |3_+\rangle \rightarrow |1\rangle$ and $|1\rangle \rightarrow |2\rangle \rightarrow |3_-\rangle \rightarrow |1\rangle$ coexist in the presence of the three electromagnetic fields. Thereby, the four-level model with two cyclic three-level substructures is formed (see Fig. 1) for the symmetric-top chiral molecule. Note that the working states and the electromagnetic fields used here are different from those for asymmetric-top chiral molecules in Refs. [49,50]. In particular, it is necessary to involve the circularly polarized electromagnetic fields for the symmetric-top chiral molecules here, but not for the asymmetric-top chiral molecules in Refs. [49,50].

The corresponding Hamiltonian reads

$$H = \omega_1 |1\rangle\langle 1| + \omega_2 |2\rangle\langle 2| + \omega_3(|3_+\rangle\langle 3_+| + |3_-\rangle\langle 3_-|)$$

$$+ [\Omega_{3_+2} e^{-i\omega_{23}t}|3_+\rangle\langle 2| + \Omega_{3_+1} e^{-i\omega_{13}t}|3_+\rangle\langle 1|$$

$$+ \Omega_{3_-2} e^{-i\omega_{23}t}|3_-\rangle\langle 2| + \Omega_{3_-1} e^{-i\omega_{13}t}|3_-\rangle\langle 1|$$

$$+ \Omega_{21} e^{-i\omega_{12}t}|2\rangle\langle 1| + \text{H.c.}], \quad (6)$$

with the coupling strengths

$$\Omega_{21} = \frac{\sqrt{3}}{6} E_{12}^s e^{-i\varphi_{12}} \langle v_2 | \hat{\mu}_z^m | v_1 \rangle,$$

$$\Omega_{3_+2} = \frac{1}{4} E_{23}^s e^{-i\varphi_{23}} \langle v_3 | \hat{\mu}_x^m | v_2 \rangle,$$

$$\Omega_{3_-2} = \frac{i}{4} E_{23}^s e^{-i\varphi_{23}} \langle v_3 | \hat{\mu}_y^m | v_2 \rangle,$$

$$\Omega_{3_+1} = i\frac{\sqrt{3}}{6} E_{13}^s e^{-i\varphi_{13}} \langle v_3 | \hat{\mu}_y^m | v_1 \rangle,$$

$$\Omega_{3_-1} = \frac{\sqrt{3}}{6} E_{13}^s e^{-i\varphi_{13}} \langle v_3 | \hat{\mu}_x^m | v_1 \rangle. \quad (7)$$

The chirality dependence of the four-level model can be seen from Eq. (7). For example, in the cyclic three-level substructure $|1\rangle \rightarrow |2\rangle \rightarrow |3_+\rangle \rightarrow |1\rangle$, the product of three transition electric dipole moments in the molecule-fixed frame ($\langle v_2 | \hat{\mu}_z^m | v_1 \rangle \langle v_3 | \hat{\mu}_x^m | v_2 \rangle \langle v_3 | \hat{\mu}_y^m | v_1 \rangle$) of the enantiomer differs in sign and reflects the chirality [40–45,47]. Hence, it is convenient to observe the chirality dependence of the four-level model due to the choice of the working states $|3_+\rangle$ and $|3_-\rangle$. In addition, the transition electric dipole moments in the molecule-fixed frame should be nonzero. Thus, we need to choose three suitable vibrational wave functions $|v_l\rangle$ ($l = 1, 2, 3$) for the working states in Eq. (4).

IV. VIBRATIONAL WAVE FUNCTION FOR THE D$_2$S$_2$ MOLECULE

For the D$_2$S$_2$ molecule, since two of its three rotational constants are almost equal ($A/2\pi = 76.15$ GHz, $B/2\pi = 6.401$ GHz, and $C/2\pi = 6.399$ GHz) [58], the states $(|1, 1\rangle + |1, -1\rangle)/\sqrt{2}$ and $(|1, 1\rangle - |1, -1\rangle)/\sqrt{2}$ of (J, K)-level structures are approximately degenerate. Then the D$_2$S$_2$ molecule can be treated approximately as the prolate symmetric-top (accidentally symmetric) chiral molecules [39]. In what follows, we take the D$_2$S$_2$ molecule as an example of symmetric-top chiral molecules to introduce how to choose the vibrational wave functions of the working states in the four-level model. It must be ensured that all the transition electric dipole moments in the molecule-fixed frame in Eq. (7) are nonzero and the product of three transition electric dipole moments of each cyclic three-level substructure differs in sign with enantiomers of the D$_2$S$_2$ molecule.

We are interested in the potential energy surface of the configuration space as a function of the following two coordinates introduced in Ref. [58]. One coordinate is the dihedral angle τ between two DSS planes, which describes the twist around the SS bond. The other coordinate is the asymmetric S-D stretching motion $\chi = R_1 - R_2$ (R_1 and R_2 are the lengths of two S-D bonds, respectively). The potential energy surfaces for τ and χ are in the form of a two-dimensional double well. The coordinate τ reflects the chirality. The left-handed states (expressed by the superscript L) are localized on the left-handed part ($0 \leqslant \tau < \pi$) of the potential energy surface and the right-handed states (expressed by the superscript R) are localized on the right-handed part ($\pi \leqslant \tau < 2\pi$). In the following, we only consider the chiral states.

We use $|\tilde{m}\rangle_\tau^Q$ and $|\tilde{n}^\pm\rangle_\chi$ to represent the eigenstates for the degrees of freedom τ and χ, respectively. Here $Q = L, R$ represents the chirality and is related to the range of τ. In addition, $\tilde{m}$ and $\tilde{n}$ are the non-negative integers and increase in unit steps. Further, $|\tilde{n}^+\rangle_\chi$ ($|\tilde{n}^-\rangle_\chi$) refers to the state with even (odd) parity for χ. Moreover, it is reasonable to assume that the eigenstates $|\tilde{m}\rangle_\tau^Q$ and $|\tilde{n}^\pm\rangle_\chi$ are dynamically decoupled [58]; then the vibrational wave functions can be written as a product of $|\tilde{m}\rangle_\tau^Q$ and $|\tilde{n}^\pm\rangle_\chi$, i.e., $|v\rangle_Q \equiv |\tilde{m}\rangle_\tau^Q \otimes |\tilde{n}^\pm\rangle_\chi$. The transition electric dipole in the molecule-fixed frame in Eq. (7) can be demonstrated as the integral over the surface of configuration space

$$_\chi\langle\tilde{n}^\pm| \otimes {}_\tau^Q\langle\tilde{m}|\hat{\mu}_{\sigma'}^m|\tilde{m}'\rangle_\tau^Q \otimes |\tilde{n}'^\pm\rangle_\chi$$
$$= \iint \psi_{\tilde{m},\tilde{n}^\pm}^{Q*}(\tau,\chi)\mu_{\sigma'}^m(\tau,\chi)\psi_{\tilde{m}',\tilde{n}'^\pm}^Q(\tau,\chi)d\tau\,d\chi, \quad (8)$$

with $\mu_{\sigma'}^m(\tau,\chi) = \langle\tau,\chi|\hat{\mu}_{\sigma'}^m|\tau,\chi\rangle$ the component of $\hat{\mu}_{\sigma'}^m$ in the representation of $|\tau,\chi\rangle$ and $\psi_{\tilde{m},\tilde{n}^\pm}^Q(\tau,\chi) = \langle\tau,\chi|\tilde{m}\rangle_\tau^Q \otimes |\tilde{n}^\pm\rangle_\chi$ the wave function of the state $|\tilde{m}\rangle_\tau^Q \otimes |\tilde{n}^\pm\rangle_\chi$ in the representation of $|\tau,\chi\rangle$.

The symmetrical relationships of $\mu_{\sigma'}^m(\tau,\chi)$ and $\psi_{\tilde{m},\tilde{n}^\pm}^Q(\tau,\chi)$ with respect to the coordinate χ are [58]

$$\mu_z^m(\tau,\chi) = \mu_z^m(\tau,-\chi),$$
$$\mu_{x,y}^m(\tau,\chi) = -\mu_{x,y}^m(\tau,-\chi),$$
$$\psi_{\tilde{m},\tilde{n}^+}^Q(\tau,\chi) = \psi_{\tilde{m},\tilde{n}^+}^Q(\tau,-\chi),$$
$$\psi_{\tilde{m},\tilde{n}^-}^Q(\tau,\chi) = -\psi_{\tilde{m},\tilde{n}^-}^Q(\tau,-\chi). \quad (9)$$

Due to the symmetrical relationships in Eq. (9), the selection of $|\tilde{n}^+\rangle_\chi$ or $|\tilde{n}^-\rangle_\chi$ plays a key role in determining whether the transition electric dipoles in the molecule-fixed frame $\langle v_j|\hat{\mu}_{\sigma'}^m|v_l\rangle$ in Eq. (7) are zero. All the nonzero transition electric dipoles in the molecule-fixed frame are

$$_\chi\langle\tilde{n}^+| \otimes {}_\tau^Q\langle\tilde{m}|\hat{\mu}_z^m|\tilde{m}'\rangle_\tau^Q \otimes |\tilde{n}'^+\rangle_\chi \neq 0,$$
$$_\chi\langle\tilde{n}^-| \otimes {}_\tau^Q\langle\tilde{m}|\hat{\mu}_z^m|\tilde{m}'\rangle_\tau^Q \otimes |\tilde{n}'^-\rangle_\chi \neq 0,$$
$$_\chi\langle\tilde{n}^+| \otimes {}_\tau^Q\langle\tilde{m}|\hat{\mu}_{x,y}^m|\tilde{m}'\rangle_\tau^Q \otimes |\tilde{n}'^-\rangle_\chi \neq 0. \quad (10)$$

Thus, a suitable set of vibrational wave functions for the working states can be selected, such as $|v_1\rangle_Q = |0\rangle_\tau^Q \otimes |0^+\rangle_\chi$, $|v_2\rangle_Q = |1\rangle_\tau^Q \otimes |0^+\rangle_\chi$, and $|v_3\rangle_Q = |1\rangle_\tau^Q \otimes |0^-\rangle_\chi$.

The symmetrical relationships of $\mu_{\sigma'}^m(\tau,\chi)$ and $\psi_{\tilde{m},\tilde{n}^\pm}^Q(\tau,\chi)$ with respect to τ are

$$\mu_z^m(\pi-\tau,\chi) = -\mu_z^m(\pi+\tau,\chi),$$
$$\mu_{x,y}^m(\pi-\tau,\chi) = \mu_{x,y}^m(\pi+\tau,\chi),$$
$$\psi_{\tilde{m},\tilde{n}^+}^L(\pi-\tau,\chi) = \psi_{\tilde{m},\tilde{n}^+}^R(\pi+\tau,\chi),$$
$$\psi_{\tilde{m},\tilde{n}^-}^L(\pi-\tau,\chi) = \psi_{\tilde{m},\tilde{n}^-}^R(\pi+\tau,\chi). \quad (11)$$

The symmetrical relationships in Eq. (11) determine the chirality dependence of the transition electric dipole in the molecule-fixed frame in Eq. (7), that is,

$$_L\langle v_2|\hat{\mu}_z^m|v_1\rangle_L = -_R\langle v_2|\hat{\mu}_z^m|v_1\rangle_R,$$
$$_L\langle v_3|\hat{\mu}_{x,y}^m|v_1\rangle_L = _R\langle v_3|\hat{\mu}_{x,y}^m|v_1\rangle_R,$$
$$_L\langle v_3|\hat{\mu}_{x,y}^m|v_2\rangle_L = _R\langle v_3|\hat{\mu}_{x,y}^m|v_2\rangle_R. \quad (12)$$

Therefore, the chirality dependence of chiral molecules reflects in the coupling strengths in Eq. (6), that is,

$$\Omega_{3_+1}^L = \Omega_{3_+1}^R = \Omega_{3_+1}, \quad \Omega_{3_-1}^L = \Omega_{3_-1}^R = \Omega_{3_-1},$$
$$\Omega_{3_+2}^L = \Omega_{3_+2}^R = \Omega_{3_+2}, \quad \Omega_{3_-2}^L = \Omega_{3_-2}^R = \Omega_{3_-2},$$
$$\Omega_{21}^L = -\Omega_{21}^R = \Omega_{21}. \quad (13)$$

Here we have added the superscript L or R to denote the left-handed or right-handed chiral molecule. In the following, when referring to left-handed (right-handed) chiral molecules, we will add the superscript. When there is no superscript, we refer to general molecules. Hence, when enantiomers couple with the same electric fields, the related coupling strengths $\pm\Omega_{21}$ reflect the chiral difference.

V. ENANTIOSPECIFIC STATE TRANSFER

In the above four-level model described by Eq. (6) (see Fig. 1), the one-photon process $|1\rangle \to |2\rangle$ is chirality dependent, while the two-photon process $|1\rangle \to |3_+\rangle \to |2\rangle$ or $|1\rangle \to |3_-\rangle \to |2\rangle$ is chirality independent. Then the interference between the one-photon process and the two-photon process in the cyclic three-level substructure is chirality dependent. Such chirality-dependent interferences give rise to the chirality-dependent dynamics for the enantiomer to achieve the enantiospecific state transfer (or the enantiodetection and enantioseparation).

Since the dynamics of the four-level model of symmetric-top chiral molecules is different from that of the cyclic three-level model, the schemes [18–24] of the enantiospecific state transfer based on the cyclic three-level models may no longer be applicable. Based on the four-level model, we will introduce two dynamic ways to achieve the enantiospecific state transfer for symmetric-top chiral molecules.

Under the three-photon resonance condition $\omega_{12} + \omega_{23} - \omega_{13} = 0$, the Hamiltonian (6) can be rewritten in the time-independent form in the interaction picture as

$$H' = \Delta_{12}|2\rangle\langle 2| + \Delta_{13}(|3_+\rangle\langle 3_+| + |3_-\rangle\langle 3_-|)$$
$$+ [\Omega_{21}|2\rangle\langle 1| + \Omega_{3_+2}|3_+\rangle\langle 2| + \Omega_{3_+1}|3_+\rangle\langle 1|$$
$$+ \Omega_{3_-2}|3_-\rangle\langle 2| + \Omega_{3_-1}|3_-\rangle\langle 1| + \text{H.c.}], \quad (14)$$

with the detunings $\Delta_{lj} \equiv (\omega_j - \omega_l) - \omega_{lj}$. We now consider the case that the electromagnetic field $\mathbf{E}_{12}^s$ is resonant with the transition $|1\rangle \leftrightarrow |2\rangle$, i.e., $\Delta_{12} = 0$. Then the other two electromagnetic fields $\mathbf{E}_{23}^s$ and $\mathbf{E}_{13}^s$ are in two-photon resonance, i.e., $\Delta_{23} = \Delta_{13} = \Delta$. Therefore, the enantiospecific state transfer can be realized by adjusting the electromagnetic fields (the field amplitudes and the phases) and the detuning.

A. Effective two-level model

In what follows, for the sake of simplicity, we assume the large-detuning condition

$$|\Delta| \gg |\Omega_{3_+1}| \sim |\Omega_{3_+2}| \gg |\Omega_{21}|,$$
$$|\Delta| \gg |\Omega_{3_-1}| \sim |\Omega_{3_-2}| \gg |\Omega_{21}| \quad (15)$$

so that the four-level model can reduce to an effective two-level one by eliminating adiabatically the excited levels

Left-handed: Right-handed:
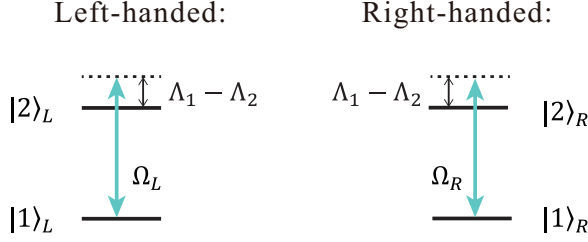
FIG. 2. Effective two-level model with the same effective detunings $\Lambda_1 - \Lambda_2$ and the chirality-dependent effective couplings $\Omega_L = \Omega_{\text{eff}} + \Omega_{21}$ for the left-handed chiral molecules and $\Omega_R = \Omega_{\text{eff}} - \Omega_{21}$ for the right-handed chiral molecules.

$|3_+\rangle$ and $|3_-\rangle$. To this end, we decompose the Hamiltonian as $H' = H_0 + H_1 + H_2$ with the zeroth-order Hamiltonian $H_0 = \Delta(|3_+\rangle\langle 3_+| + |3_-\rangle\langle 3_-|)$, the first-order term $H_1 = \Omega_{3_+2}|3_+\rangle\langle 2| + \Omega_{3_+1}|3_+\rangle\langle 1| + \Omega_{3_-2}|3_-\rangle\langle 2| + \Omega_{3_-1}|3_-\rangle\langle 1| +$ H.c., and the second-order term $H_2 = \Omega_{21}|2\rangle\langle 1| +$ H.c. By the unitary transformation $\exp(S)$ with the anti-Hermitian operator $S = (\Omega_{3_+2}|3_+\rangle\langle 2| + \Omega_{3_+1}|3_+\rangle\langle 1| + \Omega_{3_-2}|3_-\rangle\langle 2| + \Omega_{3_-1}|3_-\rangle\langle 1| -$ H.c.$)/\Delta$ [33,36,59,60], we can obtain the effective Hamiltonian $H_{\text{eff}} = \exp(-S)H'\exp(S) \simeq H_0 + [H_1, S]/2 + H_2$, which reads

$$H_{\text{eff}} = \Lambda_1|1\rangle\langle 1| + \Lambda_2|2\rangle\langle 2| + [(\Omega_{\text{eff}} + \Omega_{21})|2\rangle\langle 1| + \text{H.c.}]$$
$$+ \Delta(|3_+\rangle\langle 3_+| + |3_-\rangle\langle 3_-|) + (\Omega'_{\text{eff}}|3_+\rangle\langle 3_-| + \text{H.c.}),$$
$$(16)$$

with the energy shifts $\Lambda_1 = -(|\Omega_{3_+1}|^2 + |\Omega_{3_-1}|^2)/\Delta$ and $\Lambda_2 = -(|\Omega_{3_+2}|^2 + |\Omega_{3_-2}|^2)/\Delta$ and the effective couplings $\Omega_{\text{eff}} = -(\Omega_{3_+1}\Omega^*_{3_+2} + \Omega_{3_-1}\Omega^*_{3_-2})/\Delta$ and $\Omega'_{\text{eff}} = (\Omega^*_{3_+1}\Omega_{3_-1} + \Omega^*_{3_+2}\Omega_{3_-2})/\Delta$. In addition, the nonzero Ω_{eff} requires the vibrational wave functions of the working state to satisfy the condition of $|v_1\rangle \neq |v_2\rangle$.

In Eq. (16), the states $|3_+\rangle$ and $|3_-\rangle$ are decoupled from the states $|1\rangle$ and $|2\rangle$. That means we get an effective two-level model in the subspace $\{|1\rangle, |2\rangle\}$. Then, according to the chirality dependence of chiral molecules in Eq. (13), the effective Hamiltonian for the enantiomer in the subspace $\{|1\rangle_Q, |2\rangle_Q\}$ $(Q = L, R)$ reads

$$H^{\text{eff}}_{12,Q} = \tfrac{1}{2}(\Lambda_1 - \Lambda_2)(|1\rangle_{QQ}\langle 1| - |2\rangle_{QQ}\langle 2|)$$
$$+ (\Omega_Q|2\rangle_{QQ}\langle 1| + \text{H.c.}),$$
$$(17)$$

with the same effective detunings $\Lambda_1 - \Lambda_2$ and chirality-dependent effective couplings $\Omega_L = \Omega_{\text{eff}} + \Omega_{21}$ $(\Omega_R = \Omega_{\text{eff}} - \Omega_{21})$ for the left-handed (right-handed) chiral molecules (see Fig. 2).

B. Dynamics of the enantiospecific state transfer

It is assumed that all the molecules are initially in the ground state of the system, i.e., $|\Psi(0)\rangle_Q = |1\rangle_Q$. Then the possibility of exciting them into state $|2\rangle_Q$ can be solved analytically according to the Schrödinger equation $i\partial_t|\Psi(t)\rangle_Q = H^{\text{eff}}_{12,Q}|\Psi(t)\rangle_Q$ as

$$P^Q_2(t) = \left|\frac{\Omega_Q}{\tilde{\Omega}_Q}\right|^2 \sin^2(\tilde{\Omega}_Q t). \qquad (18)$$
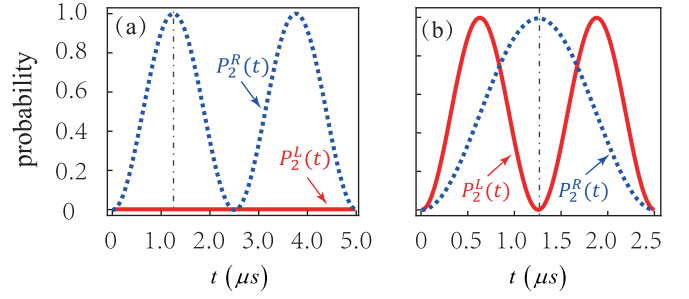
FIG. 3. Dynamic ways of the enantiospecific state transfer for symmetric-top chiral molecules based on Eq. (17) for (a) the first way with $\Omega_{21} = -\Omega_{\text{eff}} = -2\pi \times 0.10$ MHz and (b) the second way with $\Omega_{21} = 3\Omega_{\text{eff}} = 2\pi \times 0.30$ MHz. The probability occupying the state $|2\rangle_L$ $(|2\rangle_R)$ of the left-handed (right-handed) chiral molecules, $P^L_2(t)$ $[P^R_2(t)]$, is denoted by the red solid (blue dashed) line.

Here $\tilde{\Omega}_Q = \sqrt{|\Omega_Q|^2 + (\Lambda_1 - \Lambda_2)^2/4}$ and $2\tilde{\Omega}_Q$ is the Rabi oscillation frequency of the probability of occupying the state $|2\rangle_Q$. The corresponding Rabi oscillation period is $T_Q = \pi/\tilde{\Omega}_Q$.

By adjusting the effective detunings and the chirality-dependent effective couplings, enantiomers prepared initially in the same energy levels can be evolved to different energy levels, i.e., the achievement of the enantiospecific state transfer. In what follows, we will show two dynamic ways of achieving the enantiospecific state transfer. For simplicity, we will choose $\Lambda_1 = \Lambda_2$. That means $\tilde{\Omega}_Q = |\Omega_Q|$ and $T_Q = \pi/|\Omega_Q|$.

For the first way, the left-handed chiral molecules always remain in the initial state $|1\rangle_L$ while the right-handed chiral molecules experience a half-integer period of its Rabi oscillation. Then the perfect enantiospecific state transfer is achieved at $t = (N + 1/2)T_R$, with N a natural number. For this purpose, the three electromagnetic fields should be appropriately adjusted so that

$$\Omega_{21} = -\Omega_{\text{eff}}. \qquad (19)$$

Figure 3(a) illustrates an example of the first way with the parameters $\Omega_{21} = -\Omega_{\text{eff}} = -2\pi \times 0.10$ MHz based on Eq. (17). It shows that the perfect enantiospecific state transfer is achieved at $t = 1.25$ μs. Similarly, the right-handed chiral molecules always remain in the initial state $|1\rangle_R$ while the left-handed chiral molecules experience a half-integer period of its Rabi oscillation. At $t = (N + 1/2)T_L$, the perfect enantiospecific state transfer is realized.

For the second way, when the left- and right-handed chiral molecules simultaneously experience half-integer and integer periods of their corresponding Rabi oscillations, i.e.,

$$N_L T_L = \left(N_R + \tfrac{1}{2}\right)T_R, \qquad (20)$$

with $N_{L,R}$ a natural number, the perfect enantiospecific state transfer is achieved at $t = N_L T_L$. For this purpose, the three electromagnetic fields should be appropriately adjusted. Taking the case of $\Omega_{21} > \Omega_{\text{eff}} > 0$ as an example, we could adjust the three electromagnetic fields to meet

$$\Omega_{21} = \frac{2N_L + 2N_R + 1}{2N_L - 2N_R - 1}\Omega_{\text{eff}}. \qquad (21)$$

Figure 3(b) illustrates an example of the second way with the parameters $\Omega_{21} = 3\Omega_{\mathrm{eff}} = 2\pi \times 0.30$ MHz based on Eq. (17). It shows that the perfect enantiospecific state transfer is achieved at $t = 1.25 \mu$s. Similarly, when $(N_L + 1/2)T_L = N_R T_R$, the left-handed chiral molecules experience half-integer periods and simultaneously the right-handed chiral molecules experience integer periods of its Rabi oscillation. Then the perfect enantiospecific state transfer is realized at $t = N_R T_R$.

The above two ways of perfect enantiospecific state transfer are based on Eq. (17), which is obtained by adiabatically eliminating the excited states $|3_+\rangle$ and $|3_-\rangle$ in the original Hamiltonian (14). Thus, these two dynamic ways to achieve the enantiospecific state transfer for symmetric-top chiral molecules are approximately perfect.

VI. CONCLUSION

We have focused on achieving the enantiospecific state transfer for gaseous symmetric-top chiral molecules. We took the D_2S_2 molecule, which can be treated approximately as the prolate symmetric-top (accidentally symmetric) chiral molecules [39], as an example to demonstrate our method. In fact, our model and method are also applicable for the oblate symmetric-top chiral molecules ($A = B > C$), though we have just investigated the case of the prolate symmetric-top chiral molecules ($A > B = C$).

In conclusion, according to the electric dipole selection rules between the rovibrational states of symmetric-top chiral molecules, we selected the appropriate working states as well as corresponding three electromagnetic fields and then constructed a real four-level model via electric dipole transitions. Such a four-level model reflects different dynamics for enantiomers, which guarantees the achievement of the enantiospecific state transfer, enantiodetection, and enantioseparation. Further, we reduced the four-level model to the effective two-level one with the same effective detuning but the chirality-dependent effective couplings under the large-detuning condition. Then we used two dynamic ways to achieve the approximately perfect enantiospecific state transfer for symmetric-top chiral molecules when all the molecules are initially in the ground state of the system. The investigations of enantiodetection, enantioseparation, and enantioconversion [15–34] of chiral molecules are always meaningful and challenging tasks. Our four-level model will play an important role in future investigations of these issues for symmetric-top chiral molecules.

ACKNOWLEDGMENTS

[1] H. P. Latscha, U. Kazmaier, and H. A. Klein, *Organische Chemie*, 6th ed. (Springer, Berlin, 2008).

[2] A. J. Hutt and S. C. Tan, Drug chirality and its clinical significance, Drugs **52**, 1 (1996).

[3] J. Gal, The discovery of stereoselectivity at biological receptors: Arnaldo Piutti and the taste of the asparagine enantiomers-history and analysis on the 125th anniversary, Chirality **24**, 959 (2012).

[4] P. Barcellona, R. Passante, L. Rizzuto, and S. Y. Buhmann, Dynamical Casimir-Polder interaction between a chiral molecule and a surface, Phys. Rev. A **93**, 032508 (2016).

[5] P. Barcellona, H. Safari, A. Salam, and S. Y. Buhmann, Enhanced Chiral Discriminatory van der Waals Interactions Mediated by Chiral Surfaces, Phys. Rev. Lett. **118**, 193401 (2017).

[6] E. Gershnabel and I. Sh. Averbukh, Orienting Asymmetric Molecules by Laser Fields with Twisted Polarization, Phys. Rev. Lett. **120**, 083204 (2018).

[7] A. A. Milner, J. A. M. Fordyce, I. MacPhail-Bartley, W. Wasserman, V. Milner, I. Tutunnikov, and I. S. Averbukh, Controlled Enantioselective Orientation of Chiral Molecules with an Optical Centrifuge, Phys. Rev. Lett. **122**, 223201 (2019).

[8] K. A. Forbes and D. L. Andrews, Optical orbital angular momentum: Twisted light and chirality, Opt. Lett. **43**, 435 (2018).

[9] A. Yachmenev and S. N. Yurchenko, Detecting Chirality in Molecules by Linearly Polarized Laser Fields, Phys. Rev. Lett. **117**, 033001 (2016).

[10] S. N. Yurchenko, A. Yachmenev, W. Thiel, O. Baum, T. F. Giesen, V. V. Melnikov, and P. Jensen, An *abinitio* calculation of the vibrational energies and transition moments of HSOH, J. Mol. Spectrosc. **257**, 57 (2009).

[11] R. P. Cameron, S. M. Barnett, and A. M. Yao, Discriminatory optical force for chiral molecules, New J. Phys. **16**, 013020 (2014).

[12] D. S. Bradshaw and D. L. Andrews, Chiral discrimination in optical trapping and manipulation, New J. Phys. **16**, 103021 (2014).

[13] T. Wu, J. Ren, R. Wang, and X. Zhang, Competition of chiroptical effect caused by nanostructure and chiral molecules, J. Phys. Chem. C **118**, 20529 (2014).

[14] M. Shapiro, E. Frishman, and P. Brumer, Coherently Controlled Asymmetric Synthesis with Achiral Light, Phys. Rev. Lett. **84**, 1669 (2000).

[15] M. Shapiro and P. Brumer, Controlled photon induced symmetry breaking: Chiral molecular products from achiral precursors, J. Chem. Phys. **95**, 8658 (1991).

[16] A. Salam and W. Meath, On enantiomeric excesses obtained from racemic mixtures by using circularly polarized pulsed lasers of varying durations, Chem. Phys. **228**, 115 (1998).

[17] Y. Fujimura, L. González, K. Hoki, J. Manz, and Y. Ohtsuki, Selective preparation of enantiomers by laser pulses: Quantum model simulation for H$_2$POSH, Chem. Phys. Lett. **306**, 1 (1999).

[18] P. Král, I. Thanopulos, M. Shapiro, and D. Cohen, Two-Step Enantio-Selective Optical Switch, Phys. Rev. Lett. **90**, 033001 (2003).

[19] P. Král and M. Shapiro, Cyclic Population Transfer in Quantum Systems with Broken Symmetry, Phys. Rev. Lett. **87**, 183002 (2001).

[20] Y. Li and C. Bruder, Dynamic method to distinguish between left- and right-handed chiral molecules, Phys. Rev. A **77**, 015403 (2008).

[21] W. Z. Jia and L. F. Wei, Distinguishing left- and right-handed molecules using two-step coherent pulses, J. Phys. B **43**, 185402 (2010).

[22] C. Ye, Q. Zhang, Y. Y. Chen, and Y. Li, Effective two-level models for highly efficient inner-state enantioseparation based on cyclic three-level systems of chiral molecules, Phys. Rev. A **100**, 043403 (2019).

[23] B. T. Torosov, M. Drewsen, and N. V. Vitanov, Efficient and robust chiral resolution by composite pulses, Phys. Rev. A **101**, 063401 (2020).

[24] J. L. Wu, Y. Wang, S. L. Su, Y. Xia, Y. Jiang, and J. Song, Discrimination of enantiomers through quantum interference and quantum Zeno effect, Opt. Express **28**, 33475 (2020).

[25] E. Hirota, Triple resonance for a three-level system of a chiral molecule, Proc. Jpn. Acad. B **88**, 120 (2012).

[26] K. K. Lehmann, *Theory of Enantiomer-Specific Microwave Spectroscopy* (Elsevier, Amsterdam, 2017).

[27] W. Z. Jia and L. F. Wei, Probing molecular chirality by coherent optical absorption spectra, Phys. Rev. A **84**, 053849 (2011).

[28] C. Ye, Q. Zhang, Y. Y. Chen, and Y. Li, Determination of enantiomeric excess with chirality-dependent ac Stark effects in cyclic three-level models, Phys. Rev. A **100**, 033411 (2019).

[29] Y.-Y. Chen, C. Ye, Q. Zhang, and Y. Li, Enantio-discrimination via light deflection effect, J. Chem. Phys. **152**, 204305 (2020).

[30] Y.-Y. Chen, C. Ye, and Y. Li, Enantio-detection via cavity-assisted three-photon processes, Opt. Express **29**, 36132 (2021).

[31] X. W. Xu, C. Ye, Y. Li, and A. X. Chen, Enantiomeric-excess determination based on nonreciprocal-transition-induced spectral-line elimination, Phys. Rev. A **102**, 033727 (2020).

[32] Y. H. Kang, Z. C. Shi, J. Song, and Y. Xia, Effective discrimination of chiral molecules in a cavity, Opt. Lett. **45**, 4952 (2020).

[33] Y. Li, C. Bruder, and C. P. Sun, Generalized Stern-Gerlach Effect for Chiral Molecules, Phys. Rev. Lett. **99**, 130403 (2007).

[34] X. Li and M. Shapiro, Theory of the optical spatial separation of racemic mixtures of chiral molecules, J. Chem. Phys. **132**, 194315 (2010).

[35] Y.-X. Liu, J. Q. You, L. F. Wei, C. P. Sun, and F. Nori, Optical Selection Rules and Phase-Dependent Adiabatic State Control in a Superconducting Quantum Circuit, Phys. Rev. Lett. **95**, 087001 (2005).

[36] Z. H. Wang, C. P. Sun, and Y. Li, Microwave degenerate parametric down-conversion with a single cyclic three-level system in a circuit-QED setup, Phys. Rev. A **91**, 043801 (2015).

[37] L. Zhou, L. P. Yang, Y. Li, and C. P. Sun, Quantum Routing of Single Photons with a Cyclic Three-Level System, Phys. Rev. Lett. **111**, 103604 (2013).

[38] R. N. Zare, *Angular Momentum* (Wiley, New York, 1988).

[39] A. Jacob and K. Hornberger, Effect of molecular rotation on enantioseparation, J. Chem. Phys. **137**, 044313 (2012).

[40] S. Eibenberger, J. Doyle, and D. Patterson, Enantiomer-Specific State Transfer of Chiral Molecules, Phys. Rev. Lett. **118**, 123002 (2017).

[41] C. Pérez, A. L. Steber, S. R. Domingos, A. Krin, D. Schmitz, and M. Schnell, Coherent enantiomer-selective population enrichment using tailored microwave fields, Angew. Chem. Int. Ed. **56**, 12512 (2017).

[42] D. Patterson, M. Schnell, and J. M. Doyle, Enantiomer-specific detection of chiral molecules via microwave spectroscopy, Nature (London) **497**, 475 (2013).

[43] D. Patterson and J. M. Doyle, Sensitive Chiral Analysis via Microwave Three-Wave Mixing, Phys. Rev. Lett. **111**, 023008 (2013).

[44] D. Patterson and M. Schnell, New studies on molecular chirality in the gas phase: Enantiomer differentiation and determination of enantiomeric excess, Phys. Chem. Chem. Phys. **16**, 11114 (2014).

[45] V. A. Shubert, D. Schmitz, D. Patterson, J. M. Doyle, and M. Schnell, Identifying enantiomers in mixtures of chiral molecules with broadband microwave spectroscopy, Angew. Chem. Int. Ed. **53**, 1152 (2014).

[46] V. A. Shubert, D. Schmitz, C. Medcraft, A. Krin, D. Patterson, J. M. Doyle, and M. Schnell, Rotational spectroscopy and three-wave mixing of 4-carvomenthenol: A technical guide to measuring chirality in the microwave regime, J. Chem. Phys. **142**, 214201 (2015).

[47] S. Lobsiger, C. Pérez, L. Evangelisti, K. K. Lehmann, and B. H. Pate, Molecular structure and chirality detection by Fourier transform microwave spectroscopy, J. Phys. Chem. Lett. **6**, 196 (2015).

[48] C. Pérez, A. L. Steber, A. Krin, and M. Schnell, State-specific enrichment of chiral conformers with microwave spectroscopy, J. Phys. Chem. Lett. **9**, 4539 (2018).

[49] C. Ye, Q. Zhang, and Y. Li, Real single-loop cyclic three-level configuration of chiral molecules, Phys. Rev. A **98**, 063401 (2018).

[50] M. Leibscher, T. F. Giesen, and C. P. Koch, Principles of enantio-selective excitation in three-wave mixing spectroscopy of chiral molecules, J. Chem. Phys. **151**, 014302 (2019).

[51] J. Lee, J. Bischoff, A. O. Hernandez-Castillo, B. Sartakov, G. Meijer, and S. Eibenberger-Arias, Quantitative study of enantiomer-specific state transfer, arXiv:2112.09058.

[52] M. Leibscher, E. Pozzoli, C. Pérez, M. Schnell, M. Sigalotti, U. Boscain, and C. P. Koch, Complete controllability despite degeneracy: Quantum control of enantiomer-specific state transfer in chiral molecules, arXiv:2010.09296.

[53] U. Boscain, E. Pozzoli, and M. Sigalotti, Classical and quantum controllability of a rotating symmetric molecule, SIAM J. Control Optim. **59**, 156 (2021).

[54] U. Boscain, E. Pozzoli, and M. Sigalotti, Reachable sets for a 3D accidentally symmetric molecule, IFAC-PapersOnLine **53**, 1943 (2020).

[55] K. K. Lehmann, Influence of spatial degeneracy on rotational spectroscopy: Three-wave mixing and enantiomeric state separation of chiral molecules, J. Chem. Phys. **149**, 094201 (2018).

[56] C. P. Koch, M. Lemeshko, and D. Sugny, Quantum control of molecular rotation, Rev. Mod. Phys. **91**, 035005 (2019).

[57] N. V. Vitanov and M. Drewsen, Highly Efficient Detection and Separation of Chiral Molecules through Shortcuts to Adiabaticity, Phys. Rev. Lett. **122**, 173202 (2019).

[58] I. Thanopulos, P. Král, and M. Shapiro, Theory of a two-step enantiomeric purification of racemic mixtures by optical means: The D_2S_2 molecule, J. Chem. Phys. **119**, 5105 (2003).

[59] H. Fröhlich, Theory of the superconducting state. I. The ground state at the absolute zero of temperature, Phys. Rev. **79**, 845 (1950).

[60] S. Nakajima, Perturbation theory in statistical mechanics, Adv. Phys. **4**, 363 (1955).